Augmenting Flight Simulator Motion Response to Turbulence

Lloyd D. Reid* and Paul A. Robinson†
University of Toronto Institute for Aerospace Studies, Toronto, Ontario, Canada

When flight simulator motion systems are tuned for acceptable response to pilot control inputs, it is found that their response to turbulence may be unduly attenuated. The motion augmentation technique described in this paper allows the designer to increase the simulator's motion response to turbulence without otherwise altering its flight characteristics. The method employs a second set of flight equations excited only by the turbulence signals. The output from these equations is added to that from the primary simulation flight equations before being fed to the motion system. A sample case is developed showing its successful application to the heave channel of the University of Toronto Institute for Aerospace Studies Flight Research Simulator.

Nomenclature

a_B^z = heave (or z-axis) acceleration of the aircraft cockpit expressed as an F_B component
F_S = simulator-fixed body axis frame
f_B = specific force at aircraft cockpit expressed in F_B components
$f(r)$ = longitudinal turbulence correlation
f_S = specific force at simulator cockpit expressed in F_S components
g_I = acceleration due to gravity expressed in F_I components
$g(r)$ = lateral turbulence correlation
j = $\sqrt{-1}$
k = $\sqrt{k_1^2 + k_2^2 + k_3^2}$
$\boldsymbol{k}$ = wavenumber expressed in cycles per meter: $[k_1\ k_2\ k_3]^T$
$N(\boldsymbol{k})$ = the Fourier transform of $\boldsymbol{n}(\boldsymbol{x})$
$\boldsymbol{n}(\boldsymbol{x})$ = three independent Gaussian white noise sources: $[n_1\ n_2\ n_3]^T$
$R_{xx}(\tau)$ = the autocorrelation function for $x(t)$ at time delay τ
r = $\sqrt{r_1^2 + r_2^2 + r_3^2}$
$\boldsymbol{r}$ = spatial separation between two points in F_I: $[r_1\ r_2\ r_3]^T$
T_1 = $[u_G\ v_G\ w_G\ p_G\ q_G\ r_G]^T$
$\boldsymbol{x}$ = spatial coordinates in F_I
z = vertical displacement of simulator in F_I
δ_{ij} = Kronecker delta
$\sigma(t)$ = modulating variable
σ^2 = turbulence intensity
$\boldsymbol{\Phi}(\boldsymbol{k})$ = turbulence spectrum function [3 × 3 matrix with elements $\Phi_{ij}(k)$]
$\Phi_{xx}(\omega)$ = power spectral density of $x(t)$
$\Phi_{xy}(\omega)$ = cross-power spectral density between $x(t)$ and $y(t)$
ω = frequency (rad/s)

Notation

$\boldsymbol{B}$ = matrix
$\boldsymbol{B}^T$ = transpose of $\boldsymbol{B}$
$\boldsymbol{b}$ = column matrix
b^z = z component of $\boldsymbol{b}$

Received March 18, 1989; revision received Aug. 18, 1989.

*Professor and Associate Director. Associate Fellow AIAA.
†Graduate Student. Member AIAA.

Introduction

ONE of the problems facing designers of modern commercial flight simulators is how to achieve realistic motion cues while remaining within the physical limitations imposed by ground-fixed motion hardware.[1] Simulators such as the one shown in Fig. 1 typically employ a complex computer algorithm based on washout filters to preferentially remove low-frequency motion signals from the output of the flight equations before passing them on to the motion-drive hardware. This, coupled with a general scaling down of all of the motion signals, tends to eliminate most of the aircraft accelerations that are likely to drive the simulator motion hardware against its mechanical stops. Unfortunately, this signal-reduction process can lead to the production of unwanted motion cues by the flight simulator. The present paper addresses one such problem associated with the simulation of aircraft motion in response to atmospheric turbulence.

When the motion-drive washout algorithms are tuned to suit the normal range of flight maneuvers carried out in a training simulator, it is found that of the six degrees of freedom in motion, heave (or vertical motion) must be severely restricted in order to prevent the motion base from hitting the limits during pullups, pushovers, flare, and touchdown. This has the unfortunate side effect of overly attenuating the heave response of the simulator to turbulence inputs. Figure 2 shows the Bode plot of a typical heave washout filter. This is a second-order high-pass filter used in the classical algorithm CW2 described in Refs. 2 and 3. Although the technique described in this paper can be applied to all six degrees of freedom, we have concentrated on heave motion because it appears to be the most critical one for jet transport flight simulators. For this class of aircraft, the heave and roll response to turbulence are often dominant. In a typical flight simulator, the roll response will be far less restricted than the heave and thus through a process of elimination, the heave response to turbulence becomes the biggest problem.

Turbulence Model

The present development employed the simulation of a Boeing 747 described in Refs. 4–6. The atmospheric turbulence was modeled by a three-dimensional spatially frozen field consisting of three velocity components.[7] This model has been further developed to generate turbulent gusts, which have all the correlations and cross correlations defined by the theory of isotropic turbulence.

From the theory of isotropic turbulence, the three-dimensional correlation tensor is[8]

$$\frac{R_{ij}(r)}{\sigma^2} = [f(r) - g(r)]\frac{r_i r_j}{r^2} + g(r)\delta_{ij} \tag{1}$$

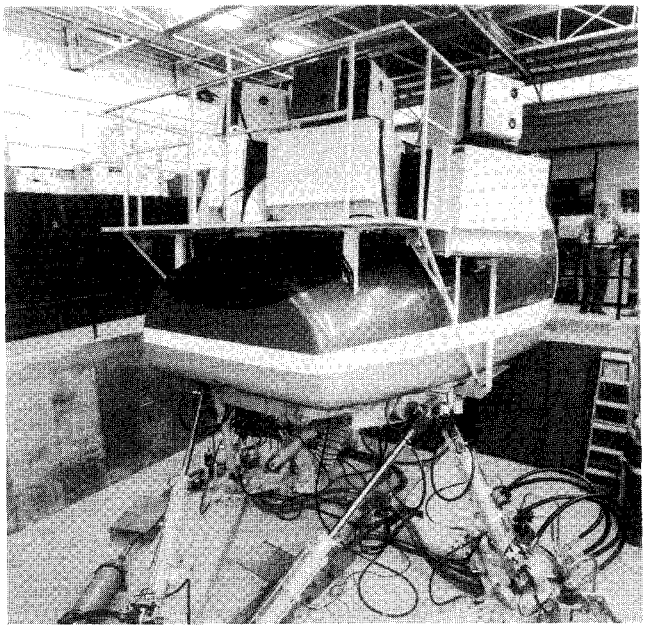

Fig. 1 UTIAS flight research simulator.

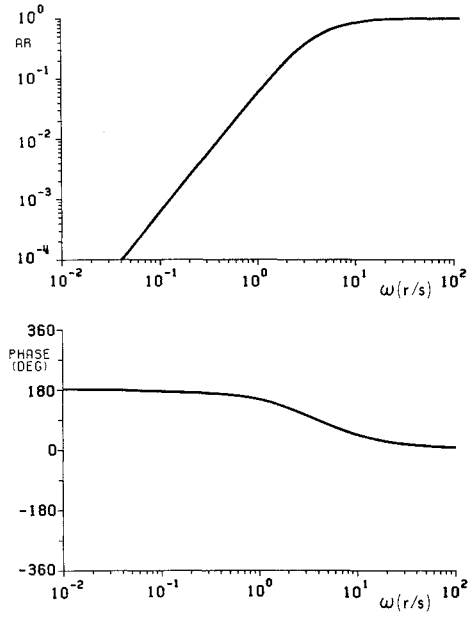

Fig. 2 CW2 heave washout filter Bode plot.

The Fourier transform of the correlation tensor yields the spectral tensor

$$\Phi_{ij}(k) = \frac{E(k)}{4\pi k^4}(k^2\delta_{ij} - k_i k_j) \tag{2}$$

where $E(k)$ is the von Kármán energy function.[9] Three turbulence velocity components are generated by

$$U(k) = G(k)\, N(k) \tag{3}$$

where $U(k)$ and $N(k)$ are the Fourier transforms of the turbulence and white noise, respectively, and the transfer function $G(k)$ comes from the solution to[10]

$$\Phi(k) = G^*(k)\, G^T(k) \tag{4}$$

with

$$G = \begin{bmatrix} G_{11} & 0 & 0 \\ G_{21} & G_{22} & 0 \\ G_{31} & G_{32} & G_{33} \end{bmatrix} \tag{5}$$

The inverse Fourier transform of $U(k)$ produces the spatial turbulence velocity field $u(x)$. As the aircraft flies through this field, the turbulence velocity at its center of gravity is determined and transformed from the ground-fixed F_I frame into the aircraft body frame F_B. In a similar manner, the significant turbulence velocity gradients are computed in F_B as well. This generates turbulence time series consisting of three velocities and three gradients, which are used to produce aircraft forces and moments.

It is generally accepted that turbulence is a non-Gaussian process.[11] In particular, its amplitude distribution tends to be patchy with significant periods of low and high intensity. The method for producing turbulence was based in the filtering of Gaussian white noise and, as a consequence, the initial turbulence field was also Gaussian. In order to increase the realism in flight simulation applications, it is necessary to alter the statistical properties of this initial turbulence while maintaining the spectral characteristics. A suitable process has been introduced in Ref. 12. Consider

$$w(t) = \sigma(t)\, z(t) \tag{6}$$

where it is desired to have the spectral properties of $w(t)$ identical to those of $z(t)$ and at the same time to have a different probability density function. This is achieved by employing a fluctuating $\sigma(t)$. It can be shown that the desired properties can be achieved when

$$\frac{d^2 R_{\sigma\sigma}(\tau)}{d\tau^2}$$

is suitably small as $\tau \to 0$. This technique has been used to process the initial turbulence field in order to generate patchy turbulence. Figure 3 depicts typical values for the velocity components in F_B (u_G, v_G, w_G) and gradients in F_B (p_G, q_G, r_G) as recorded at the aircraft's center of gravity during a simulated test flight.

All simulated test flights were carried out with the autopilot disengaged and the aircraft controls fixed. The aircraft was in its clean configuration and trimmed for straight and level flight at 400 kt true airspeed at an altitude of 21,000 ft.

Simulator Motion Augmentation

The path from turbulence input to simulator motion can be seen in Fig. 4. Ignoring the augmentation system, the inputs to the flight equations of block 1 are the pilot's controls δ, and the turbulence T_1 consisting of the preceding six components. The response of the flight equations to these inputs feeds the visual display (outside scene), the flight instruments, and the motion system. The goal of the present scheme is to augment the simulator's motion response to turbulence without interfering with the visual display and instruments. This can be achieved by generating a signal representing the aircraft's response to turbulence alone and then feeding it into the motion system in a suitable manner. Because the frequency content of motion signals due to turbulence overlaps substantially with that due to pilot control activity, it is not possible to separate the two effects through the use of filters on the output of the flight equations of block 1. The proposed technique for obtaining a signal representing the aircraft motion response due to turbulence is depicted in Fig. 4 by the augmentation system. Here T_2 represents the turbulence input (which may be the same as T_1 or different depending on the designer's goals) and the flight equations of block 2 may be the same as those of block 1 or a simplified version of them. The output from the flight equations of block 2 is used to generate turbu-

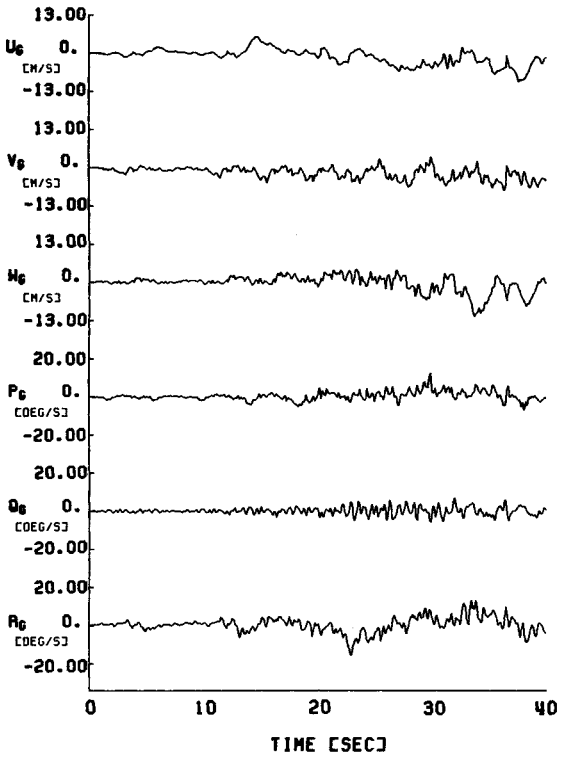

Fig. 3 Turbulence field.

lence related simulator motions by suitably adding it to the signals already present due to δ and T_1 coming from the flight equations of block 1. This is used to compensate for the undesired attenuation of the motion signal due to T_1 by the simulator's primary washout filters. Figure 5 illustrates how the augmented motion signal is introduced into the classical washout algorithm (CW2) employed in the present development. The upper path in the diagram operates on the specific force f_B. Specific force is defined as the difference between inertial acceleration a and the acceleration due to gravity g

$$f = a - g \tag{7}$$

This signal is scaled and then transformed into the ground-fixed inertial frame F_I by the transformation matrix L_{IS}. The vector g_I is then added to create an inertial acceleration signal which is passed through the high-pass filters of block HP FILT 1. The signal is then double integrated with respect to time to produce the simulator position command S_{I_1}. The motion augmentation inertial acceleration signal a_G passes through a similar chain of processing to produce the augmentation position command S_{I_2}. The final position command to the simulator motion system is S_I where

$$S_I = S_{I_1} + S_{I_2} \tag{8}$$

If the flight equations were linear differential equations, then the aircraft response due to T_1 and T_2 would be the same if $T_1 \equiv T_2$ and both sets of flight equations were identical, and the proposed scheme could be used to duplicate precisely the application of different washout filters to aircraft motions due to pilot inputs and aircraft motions due to turbulence. However, in general (and in the present case), the flight equations are nonlinear and thus nonlinear interaction results in less than exact turbulence response duplication by the motion augmentation scheme.

A further approximation may also be desirable in the interests of reduced processing time when the technique is implemented on the simulator's digital computer. This involves the selection of T_2 to include only a subset of the elements of T_1 and the use of reduced-order flight equations in block 2.

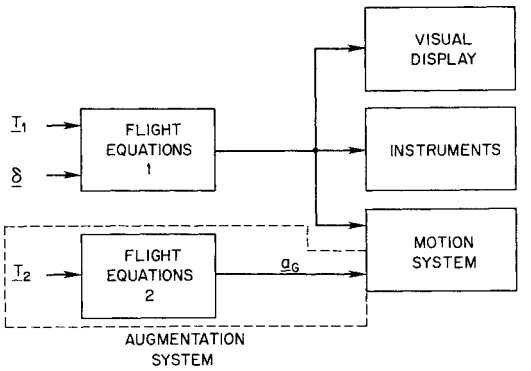

Fig. 4 Simulator system.

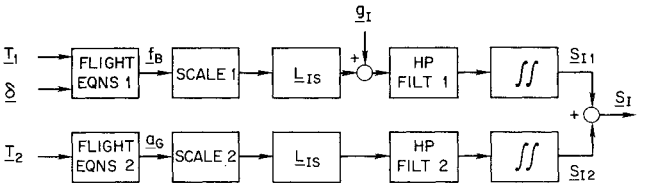

Fig. 5 CW2 motion drive algorithm.

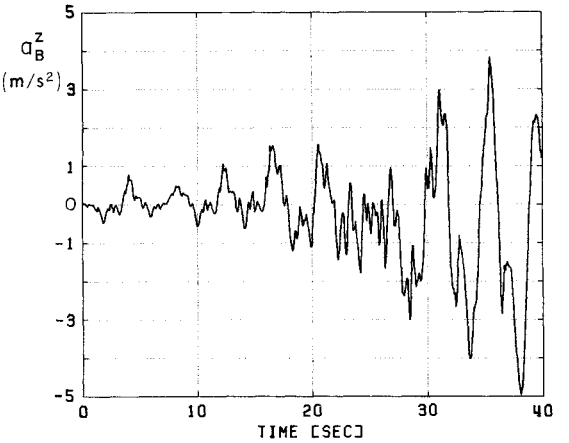

Fig. 6 Aircraft cockpit heave acceleration (using complete turbulence field).

In the present application to the heave channel, it was found that for the B-747 the dominant turbulence input was w_G. This can be seen in Figs. 6 and 7 showing the aircraft's response in vertical acceleration a_B^z (measured at the cockpit) for a controls-fixed flight through the turbulence depicted in Fig. 3. The result shown in Fig. 6 is the response when all six turbulence components are present. That of Fig. 7 is the response when only w_G is present (this was produced by feeding the aircraft equations the w_G time history found when generating Fig. 6). It can be seen that the time histories of Figs. 6 and 7 are quite similar. The corresponding measured a_B^z power spectra are plotted in Fig. 8. It can be seen that the use of w_G alone to produce a_B^z has resulted in a slight loss of power content primarily at the high-frequency end of the spectrum. Overall, however, it was concluded that for the present application, it is feasible to employ w_G alone when generating the simulator heave motion augmentation signal.

In order to minimize the computer cycle time increment caused by solving the flight equations of block 2 in Fig. 4, it was decided to employ a reduced-order set of equations. This was achieved by determining the describing function relating a_B^z to w_G and then fitting a low-order transfer function to it. A

Bode plot of this describing function was generated by using power spectral density measurements based on input (w_G) and output (a_B^z) data produced while flying through the complete turbulence field of Fig. 3 (i.e., w_G from Fig. 3 and a_B^z from Fig. 6). The describing function is given by[13]

$$DF(\omega) = \frac{\Phi_{w_G a_B^z}(\omega)}{\Phi_{w_G w_G}(\omega)} \tag{9}$$

The measured describing function is shown in Figs. 9 and 10. The degree to which this describing function accounts for the observed a_B^z can be found from the coherence function given by

$$\rho^2(\omega) = \frac{|\Phi_{w_G a_B^z}|^2}{\Phi_{w_G w_G}\Phi_{a_B^z a_B^z}} \tag{10}$$

The ρ^2 can range from 0 to 1 with 1 indicating perfect representation and 0 negligible representation. A plot of $\rho^2(\omega)$ is given in Fig. 11 where it is seen that a reasonable representation is achieved. Now in order to obtain an analytical form for the describing function, it is necessary to fit a transfer function of a particular form to the data of Figs. 9 and 10. After several different forms were investigated, it was decided that a second-order low-pass filter would be sufficiently precise for the current application. The results of the fitting process are shown by the solid curves in Figs. 9 and 10. It was decided to achieve the best fit possible to the amplitude curve on the assumption that phase-error effects would be less noticeable to

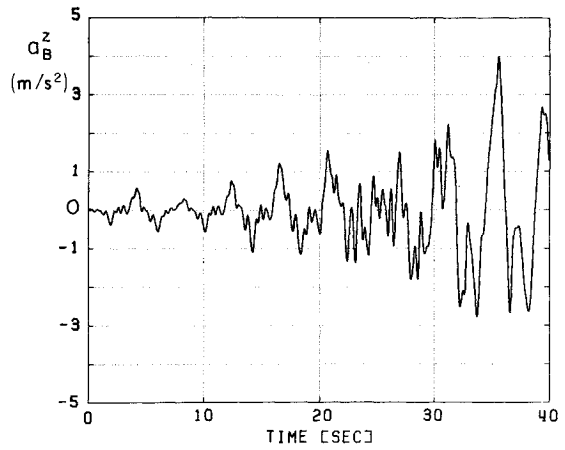

Fig. 7 Aircraft cockpit heave acceleration (using w_G alone).

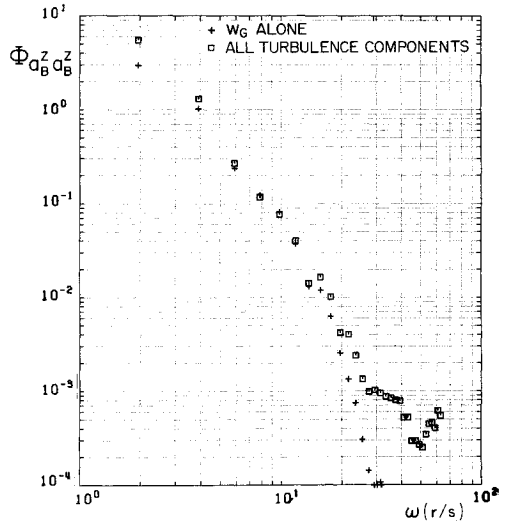

Fig. 8 Power spectral density of aircraft cockpit heave acceleration.

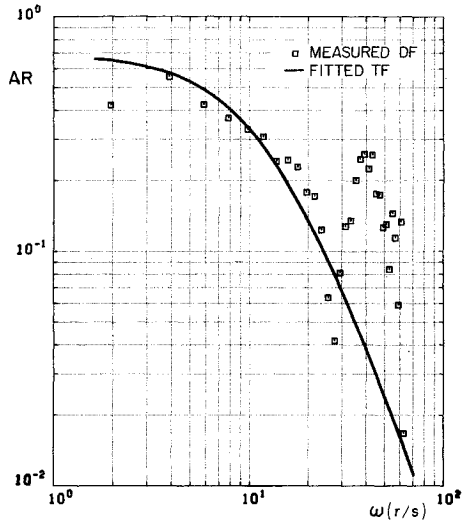

Fig. 9 Amplitude ratio of *DF* and *TF*.

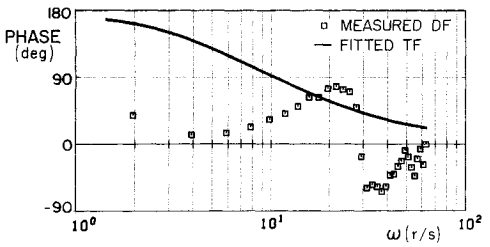

Fig. 10 Phase angle of *DF* and *TF*.

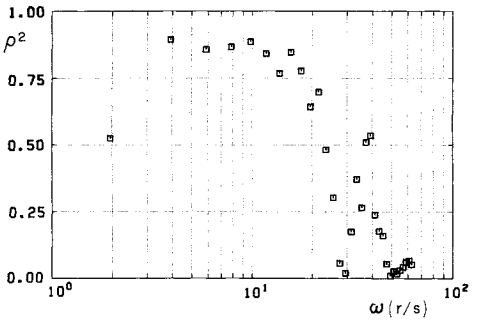

Fig. 11 Coherence function for *DF*.

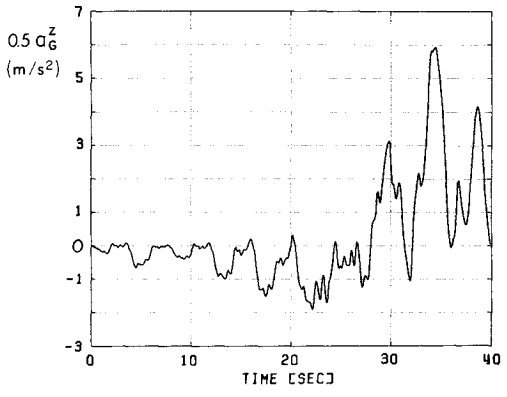

Fig. 12 Augmentation heave acceleration signal 0.5 a_G^z.

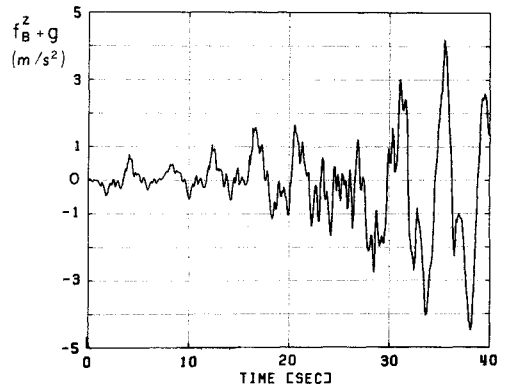

Fig. 13 Aircraft cockpit vertical specific force.

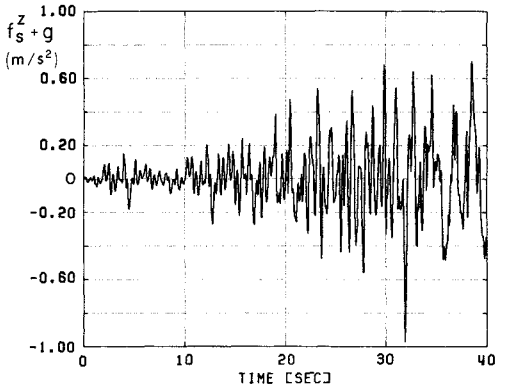

Fig. 14 Simulator cockpit vertical specific force (motion augmentation off).

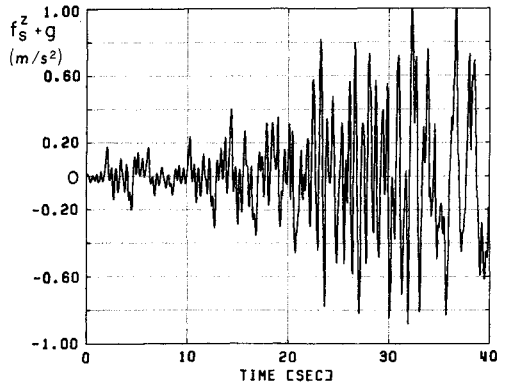

Fig. 15 Simulator cockpit vertical specific force (motion augmentation on).

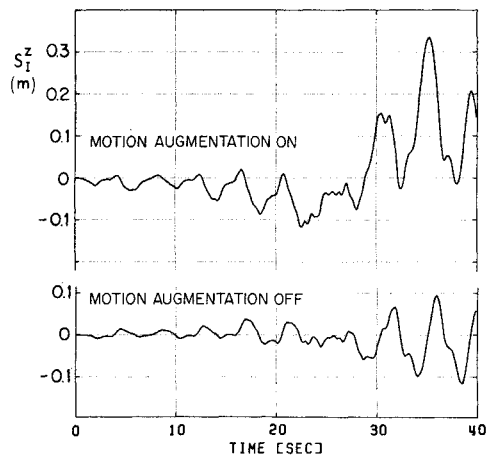

Fig. 16 Simulator vertical travel.

the pilots. The transfer function was selected to be

$$TF(\omega) = \frac{-65}{(j\omega + 10)^2} \tag{11}$$

The influence of the poor fit to the phase data will be assessed in the next section.

Evaluation of the Technique

The preceding motion augmentation scheme was implemented on the University of Toronto Institute for Aerospace Studies (UTIAS) Flight Research Simulator. The motion drive algorithm selected for the test was the classical parameter version CW2. For this initial test, the high-pass filters in the motion augmentation channel (see Fig. 5) were selected to be identical to those in the primary channel (i.e., HP FILT 1 and 2 were the same). Scaling block SCALE 2 was used to adjust the degree-of-motion augmentation achieved.

Figure 12 gives a plot of 0.5 a_G^z for $T_2 = w_G$ (the w_G shown in Fig. 3). Comparing this with the a_B^z plot of Fig. 6 it is seen that a reasonable heave acceleration response is generated.

In order to demonstrate the impact of the motion augmentation technique on the simulator response, first consider Fig. 13. This is a plot of the vertical component of specific force f_B^z in the cockpit of the simulated aircraft as it flies through the complete turbulence field. This is of interest because specific force is the translational motion sensed by the pilot's vestibular system. Figure 14 is a plot of f_S^z as generated by the simulator for the same test flight without motion augmentation. It can be seen that as expected the specific force is considerably attenuated and has much of its low-frequency content removed. Figure 15 shows the simulator response for the same test flight but with motion augmentation activated (with a scale factor of 0.5 employed in both channels of Fig. 5). When compared with Fig. 14, it can be seen that the desired increase in amplitude has been achieved. Because the same high-pass filter was used in the augmentation channel, the same low-frequency content removal is evident. Figure 16 indicates the increased simulator travel in the z direction required to support the increased activity in heave. Reducing the break frequency of the high-pass filter of the motion augmentation system would produce more low-frequency heave response to turbulence at the expense of an even greater increase in z travel.

In viewing the plots of Figs. 13–15, there is no indication that the poor fit of the augmentation system transfer function to the phase data of Fig. 10 has had a noticeably bad influence on the performance of the system. For this reason no further refinement of this transfer function was deemed necessary.

Summary

Experience with the UTIAS Flight Research Simulator while simulating a B-747 indicated that when the motion base drive algorithms are tuned so as to be well suited to typical flight maneuvers carried out by pilots during training, the resulting simulator heave response to turbulence alone is excessively attenuated. Since large-scale pilot maneuvers during flight through turbulence are unlikely, it appeared reasonable to assume that the simulator could be allowed to respond more strongly to heave induced by turbulence. A technique for achieving this has been developed and demonstrated to be effective. It alters only the simulator motion base response to turbulence, leaving unchanged its response to pilot inputs and does not alter the visual and instrument displays.

Although the technique has been demonstrated for heave alone, it can equally well be applied to other degrees of freedom. In addition, further refinements could be added whereby the flight equations of block 2 in Fig. 4 are programmed to alter their form in response to changes in the aircraft's configuration and airspeed. For example, a different form would probably be needed for the landing configuration.

At the present time, an experimental program to assess pilot opinion of the effectiveness of the technique has not been carried out, and this is a logical next step in its further development.

Acknowledgment

This project was supported by an Operating Grant provided by the Natural Sciences and Engineering Research Council of Canada.

References

[1]Jansen, C., "Present and Future Developments of the NLR Moving Base Research Flight Simulator," AIAA Paper 88-4584, Sept. 1988.

[2]Reid, L. D., and Nahon, M. A., "Flight Simulation Motion-Base Drive Algorithms: Part 1—Developing and Testing the Equations," University of Toronto, Canada, UTIAS Rept. 296, Dec. 1985.

[3]Reid, L. D., and Nahon, M. A., "Flight Simulation Motion-Base Drive Algorithms: Part 2—Selecting the System Parameters," University of Toronto, Canada, UTIAS Rept. 307, May 1986.

[4]Hanke, C. R., and Nordwall, D. R., "The Simulation of a Jumbo Jet Transport Aircraft, Volume 2: Modeling Data," NASA CR-114494, Sept. 1970.

[5] Hanke, C. R., "The Simulation of a Large Jet Transport Aircraft," NASA CR-1756, March 1971.

[6]Reid, L. D., and Nahon, M. A., "Flight Simulation Motion-Base Drive Algorithms: Part 3—Pilot Evaluations," University of Toronto, Canada, UTIAS Rept. 319, Dec. 1986.

[7]Campbell, C. W., "A Spatial Model of Wind Shear and Turbulence for Flight Simulation," NASA TP-2313, May 1984.

[8]Batchelor, G. K., *Homogeneous Turbulence,* Cambridge University Press, Cambridge, 1953.

[9]Etkin, B., *Dynamics of Atmospheric Flight,* Wiley, New York, 1972.

[10]Etkin, B., personal communication, May 1988.

[11]van de Moesdijk, G. A. J., "Non-Gaussian Structure of the Simulated Turbulent Environment in Piloted Flight Simulation," Dept. Aerospace Engineering, Delft University of Technology, The Netherlands, Memo M-304, April 1978.

[12]Press, H., "Atmospheric Turbulence Environment with a Special Reference to Continuous Turbulence," AGARD Rept. 115, April-May, 1957.

[13]Reid, L. D., "The Measurement of Human Pilot Dynamics in a Pursuit-Plus-Disturbance Tracking Task," University of Toronto, Canada, UTIAS Rept. 138, April 1969.